

## Simple Synthesis of Aminoquinoline/Ethylaniline Copolymer Semiconducting Nanoparticles

Xin-Gui Li,<sup>\*[a, b]</sup> Yi-Min Hua,<sup>[b, c]</sup> and Mei-Rong Huang<sup>\*[b]</sup>

**Abstract:** Pure copolymer nanoparticles from 8-aminoquinoline (AQ) and 2-ethylaniline (EA) were easily synthesized by a chemically oxidative polymerization in three different aqueous media. The potential and temperature of polymerization solution were used to successfully follow the polymerization progress. The molecular and morphological structures of the resulting AQ/EA copolymer particles were systematically characterized by IR, UV/Vis, NMR, gel permeation chromatography, laser particle-size analysis, atomic force and transmission electron microscopy. The oxidation potential of

the monomers as well as the polymerization yield, structure, and properties of the particles were found to significantly depend on AQ/EA ratio, polymerization temperature and medium. It is surprisingly found that AQ homopolymerization and AQ/EA (50:50) copolymerization at 5 °C in HCl simply afford nano-ellipsoids with the major/minor axis diameters of 24/14 nm and 80/67 nm, respectively. A simple

method of synthesizing semiconducting pure nanoparticles by introducing the AQ units with positively charged quaternary ammonium groups but in the absence of adsorptive stabilizer or sulfonic substituent on the monomers is established first. Both the molecular weight and bulk electroconductivity of the copolymers exhibit a maximum at AQ content of 10 mol %. The solubility and film formability of the copolymers are good in highly polar solvents and reach the optimal at the AQ content of 20 and 10 mol %, respectively.

**Keywords:** conducting materials • nanotechnology • polymers • semiconductors

### Introduction

Nitrogen heterocyclic aromatic amines can form a new type of nitrogen-containing polymer simply by a chemical or electrochemical oxidative polymerization. With primary amino group to be used for oxidative polymerization, the heterocyclic amine leaves -C=N-C- group in the ring as one more redox site than polyaniline (PAN). Therefore the ni-

trogen heterocyclic amine polymer is expected as a new electrode material that offers better electrocatalysis properties than conventional non-heterocyclic amine polymer. On the other hand, due to its linkage structural similarity to PAN, the nitrogen heterocyclic polymer also has various novel properties such as electrical semiconductivity,<sup>[1]</sup> metal ion adsorbability,<sup>[2a]</sup> trace metal ion detectability,<sup>[2b]</sup> and oxygen/nitrogen separation capability.<sup>[1,3]</sup> Thus the nitrogen heterocyclic polymer is a novel multifunctional material with a wide application potential.

As a bifunctional nitrogen heterocyclic aromatic amine, aminoquinoline has one nitrogen atom on its aromatic ring. Aminoquinoline polymer shows special properties similar to other polymers from nitrogen heterocyclic aromatic amine.<sup>[4-6]</sup> There are only a few studies on the electrochemical polymerization of quinoline and its derivatives until now.<sup>[4-6]</sup> The polymer films obtained are dense, even and tough. However, the film area and shape are strongly dependent on the size and shape of the electrode used. On the other hand, the low solubility of aminoquinoline polymers restricts their practical application. It has been reported that substituted PANs exhibit a reformative solubility and therefore a significantly improved processibility in comparison

[a] Prof. Dr. X.-G. Li  
Department of Chemistry and Chemical Biology  
Harvard University, 12 Oxford Street  
Cambridge, MA 02138 (USA)  
Fax: (+1) 617-495-4723  
E-mail: xingui@fas.harvard.edu

[b] Prof. Dr. X.-G. Li, Y.-M. Hua, Prof. M.-R. Huang  
Institute of Materials Chemistry  
School of Materials Science and Engineering  
Tongji University, 1239 Siping Road  
Shanghai 200092 (China)  
E-mail: huangmeirong@tongji.edu.cn  
lixingui@tongji.edu.cn

[c] Y.-M. Hua  
Department of Chemistry, The University of Arizona  
Tucson, AZ 85721 (USA)

with PAN.<sup>[1,7,8]</sup> As a typical aniline derivative, 2-ethylaniline (EA) has often been used to copolymerize with other aromatic monomers for a great enhancement of the polymer solubility and further the processibility.<sup>[9]</sup> Chemically oxidative copolymerization of aminoquinoline and EA may resolve these problems but no report concentrates on it so far.

Here we report a highly efficient chemical oxidative copolymerization of 8-aminoquinoline (AQ) with EA as one of the best methods to combine the advantages of the two homopolymers. The polymerization feature, structure, and properties of the AQ/EA copolymer fine particles are also described in detail. A novel simple method to synthesize the pure polymer particles with the diameter of down to ~14 nm by the oxidative polymerization in relatively pure reaction media in the absence of additives or ionic side groups as stabilizer is suggested for the first time. The function of a positively charged AQ unit for the simple formation and stable existence of the pure polymer nanoparticles is elaborated.

## Results and Discussion

**Oxidation potential of AQ and EA monomers:** On the basis of the first cyclic voltammograms during the electropolymerization of AQ, EA, and AQ/EA (50:50) mixture monomers, the oxidation potential of AQ, EA, and AQ/EA (50:50) mixture is found to be 0.91, 0.94, and 0.94 V versus saturated calomel electrode (SCE) in H<sub>2</sub>SO<sub>4</sub> aqueous solution respectively. Their oxidation potential in NaClO<sub>4</sub>/MeCN slightly reduces to 0.86, 0.87, and 0.91 V versus SCE, respectively. It appears that the oxidation potential of AQ/EA (50:50) mixture is not a simple addition of the oxidation potentials of both monomers. In addition, as mentioned above, the oxidation potentials of AQ and EA monomers are very close. Both of these imply that the oxidation of both monomers should be strongly influenced each other. In other words, the copolymerization between the AQ and EA monomers should occur rather than homopolymerization separately. Hence, a genuine copolymer containing AQ and EA units would form through the oxidative polymerization.

**Copolymerization of AQ and EA monomers:** The chemical oxidative copolymerization between AQ and EA monomers of various ratios afforded a dark precipitate as products in the three-polymerization media. The color of the products changes from black to brown with an increase in AQ content from zero to 100%. The AQ/EA copolymerization process was in situ monitored by detecting the variation of the open-circuit potential (OCP) and temperature of the polymerization solution, which might supply a deeper insight

into polymerization progress, as listed in Table 1. The initial OCP of EA monomer in 1 M HCl was 469 mV versus SCE, which was counterpoise potential for the protonated EA monomer after a time lapse of 0.5 h. After the addition of AQ monomer to the EA solution, the initial OCP of the co-

Table 1. Variation of the open-circuit potential (OCP) during polymerization of 8-aminoquinoline (AQ) and 2-ethylaniline (EA) in 1 M HCl aqueous solution at 5 °C.

AQ/EA feed molar ratio	Solution potential /mV vs SCE initial/top/ $\Delta P$ <sup>[a]</sup>	Polymerization time, $t_1/t_2$ /min	AQ/EA calcd molar ratio	<sup>1</sup> H NMR results calcd degree of polymerization of the polymers
0:100	469/745/276	9/111	0:100	32
10:90	262/577/315	40/>350	13:87	72
30:70	289/610/321	37/>600	67:33(18) <sup>[b]</sup>	61
50:50	293/631/338	68/>600	89:11(21) <sup>[b]</sup>	15
100:0	320/727/407	29/>700	100:0(23) <sup>[b]</sup>	13

[a]  $\Delta P$  = Top potential – initial potential. [b] The data in the parentheses are the molar content of quaternary ammonium structures.

monomer solution decreased to 262–320 mV versus SCE. When the oxidant [(NH<sub>4</sub>)<sub>2</sub>S<sub>2</sub>O<sub>8</sub>] solution was dropped into the AQ/EA comonomer solution, an instant OCP rise was observed. The variation of OCP with reactant concentration for the oxidative polymerization process is given by the Nernst equation:

$$\text{OCP} = E^0 + (RT/nF) \ln(c_{\text{Ox}}/c_{\text{Re}}) \quad (1)$$

where  $E^0$  is the standard electrode potential of the polymerization,  $R$  the gas constant,  $T$  the absolute temperature,  $n$  the number of electrons,  $F$  the Faraday constant,  $c_{\text{Ox}}$  and  $c_{\text{Re}}$  the concentration of the oxidized and reduced species. Obviously, the solution OCP during the polymerization will vary with oxidant [(NH<sub>4</sub>)<sub>2</sub>S<sub>2</sub>O<sub>8</sub>] and reducer [monomer] concentrations. At AQ feed content of less than 10 mol%, there are three distinct stages in the OCP-time plots, that is, an up stage, plateau and down stage. A similar situation was observed during the chemical oxidative polymerization of aniline.<sup>[10]</sup> A continuously increased OCP in first stage ( $t_1$ ) should be ascribed to dissociation of the persulfate ions to radical anions, SO<sub>4</sub><sup>•-</sup>, and anion, SO<sub>4</sub><sup>2-</sup> in the presence of monomers. In this stage, the oligomers formed can act as a reducer. The oxidized oligomers could propagate subsequent polymerization with residual monomers via an electrophilic aromatic substitution mechanism. Accompanying the OCP change, the color of the polymerization solution darkened incessantly, suggesting the formation of dark polymer precipitates.

As the copolymerization proceeded, the OCP reached an even plateau between 577 and 745 mV versus SCE. In the second step, the AQ/EA copolymer chains formed in the first step may be further oxidized by the remanent oxidant. The propagation may continue on the oxidized chains to form a higher molecular-weight polymer. These newly formed AQ/EA polymer chains may also be oxidized to participate in the chain propagation. This process is repeated

until all the oxidant is consumed at the end of the plateau stage ( $t_2$ ). After the plateau stage, the OCP declined stably. The third step ( $t_3$ ) should include further polymerization of monomers with the oxidized polymer chain that formed in the second step as the oxidant instead of  $(\text{NH}_4)_2\text{S}_2\text{O}_8$ . The time elapsed at the end of the plateau, that is,  $t_1+t_2$ , may be an indication of the polymerization rate.<sup>[10]</sup> As listed in Table 1,  $t_1+t_2$  increased with an increase in AQ content and the third step was not observed in the case of AQ homopolymerization. That is to say, the copolymerization rate slowed down with adding and increasing AQ content. One of the reasons is that the steric hindrance of the quinoline ring is greater than that of phenyl ring of EA, leading to more difficult electrophilic reaction between monomers and propagating chains. On the other hand, it is seen from Table 1 that the initial and top OCPs of the polymerization solution demonstrate a minimum at AQ feed content of 10 mol%, indicating that the OCP of AQ/EA comonomer solution is not a simply linear addition of their individual solutions. This should be an indication of a strong interaction between AQ and EA monomers, that is, a real copolymerization occurred between them.

It is seen that the AQ/EA polymerization yield is non-monotonously dependent on the monomer ratio, as shown in Figure 1. The yield decreases from the highest value of

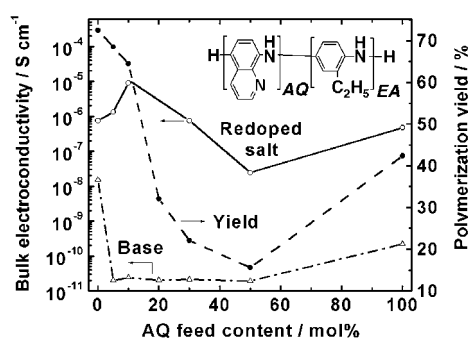


Figure 1. Nominal molecular structure of 8-aminoquinoline (AQ)/2-ethylaniline (EA) copolymers and the effect of AQ feed content on polymerization yield and bulk electrical conductivity (measured at 18°C) of AQ/EA copolymer particles prepared in 1 M HCl aqueous solution at 5°C.

72.5% to a minimum value of 15.6% as AQ feed content increases from zero to 50 mol%. With a further increase in AQ feed content to 100 mol%, the yield increases to a medium value of 42.5%. This indicates a lower copolymerizability between AQ and EA comonomers than respective EA or AQ homopolymerizability. That is to say, the chain propagations between activated EA end group and AQ monomer (or between activated AQ end group and EA monomer) are stopped by each other, that is, a retardation between EA (or AQ) end group and AQ (or EA) monomer. This retardant copolymerization finally results in a lower yield of copolymerization than that of respective homopolymerizations. It also clearly suggests a copolymerization effect or a strong interaction between AQ and EA monomers, that is, the AQ/EA polymer prepared by the chemical

oxidative polymerization is a real copolymer rather than a mixture of AQ and EA homopolymers.

It is found that the solution temperature during AQ/EA (10:90) copolymerization in HCl rises with polymerization time and attains a maximum at a certain time. The maximum temperature depends on the initial solution temperature. At the initial temperatures of 25 and 35°C, the maximum temperature reaches up to 27.5 and 41.5°C at 68 and 30 min, respectively; this suggests an exothermic copolymerization. Moreover, the higher the initial polymerization temperature, the higher the reaction exotherm is because the stronger oxidative ability of the oxidant at higher temperature can result in faster creation of active centers in the system and then faster polymerization. Therefore, a significant dependence of the copolymerization yield on the polymerization temperature is shown in Figure 2. The AQ/EA (10:90) copolymerization yield reached the highest value of

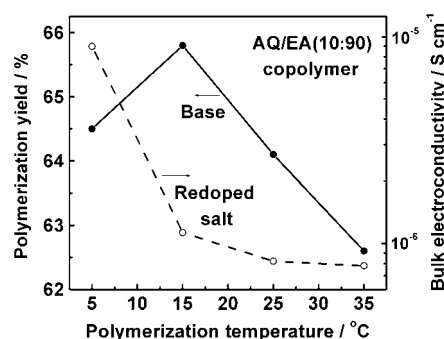


Figure 2. Influence of the polymerization temperature on the copolymerization yield of 8-aminoquinoline (AQ)/2-ethylaniline (EA) (10:90) in 1 M HCl aqueous solution and on the copolymer conductivity measured at 10°C after redoped in 1 M HCl.

65.8% at the initial reaction temperature of 15°C. A similar relationship between the yield and polymerization temperature has been observed for *p*-phenylenediamine and *o*-phenetidine copolymerization.<sup>[11]</sup> It appears that the optimized copolymerization temperature for AQ/EA (10:90) copolymer is around 15°C because the yield is the maximum at this temperature.

The chemically oxidative polymerization of aniline and other aromatic amines is based on a usually recognized radical cation mechanism in acidic medium. In this study, AQ/EA copolymer particles were also triumphantly synthesized in a neutral acid-free MeCN aqueous medium. A strong effect of polymerization medium on the AQ/EA (10:90) copolymerization is illustrated in Figure 3 and Table 2. The AQ/EA (10:90) polymerization temperature in the MeCN/water medium came to a head earlier than that in other two acidic media. It indicates that the oxidative polymerization rate of AQ and EA monomers gets higher with raising the pH value of the medium due to its stronger deprotonation effect. A similar behavior was also observed in aniline polymerization.<sup>[12]</sup> However, it appears that the polymerization yield does not change greatly with reaction medium.

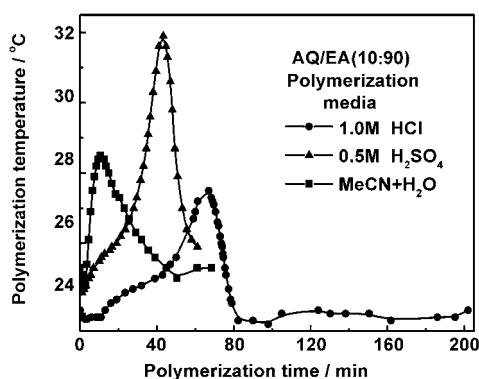


Figure 3. Temperature profile during 8-aminoquinoline (AQ)/2-ethylaniline (EA) (10:90) copolymerization at 25°C in 1 M HCl aqueous solution, 0.5 M H<sub>2</sub>SO<sub>4</sub> aqueous solution and a MeCN/H<sub>2</sub>O mixture with a volume ratio of 2:1, respectively.

Table 2. The influence of polymerization media on the polymerization yield, size and conductivity of fine particles of 8-aminoquinoline (AQ)/2-ethylaniline (EA) (10:90) copolymers prepared at 25°C.

Polymerization media	Polymerization yield/%	Particle diameter / $\mu\text{m}$		Standard deviation of the diameter / $\mu\text{m}$		Bulk electrical conductivity of 1 M HCl redoped particles/S $\text{cm}^{-1}$ at 10°C
		virgin salt	base	virgin salt	base	
1 M HCl	64.1	5.866	2.865	3.860	1.743	$8.22 \times 10^{-7}$
0.5 M H <sub>2</sub> SO <sub>4</sub>	67.3	5.143	3.209	2.921	1.778	$3.6 \times 10^{-7}$
MeCN + H <sub>2</sub> O <sup>[a]</sup>	63.7	–	3.091	–	2.543	$2.73 \times 10^{-11}$

[a] Volume ratio of MeCN to H<sub>2</sub>O 2:1.

**IR spectra of the AQ/EA copolymers:** A systematic variation of the IR spectra of the copolymer bases with AQ/EA monomer ratio is shown in Figure 4. A broad absorption at 3380  $\text{cm}^{-1}$  due to characteristic N–H stretching vibration indicates the existence of secondary amino groups. The peak at 3040  $\text{cm}^{-1}$  is ascribed to aromatic C–H stretching vibration. Three weak peaks at 2960/2920 and 2862  $\text{cm}^{-1}$  correspond to aliphatic C–H asymmetric and symmetric stretching vibrations of the ethyl groups on the EA units, respectively. With increasing AQ content, all the three peaks above-mentioned become weaker because AQ unit does not contain aliphatic C–H bond. Absorption peaks appeared at 1595 and 1500  $\text{cm}^{-1}$  are attributed to the quinoid and benzenoid rings, respectively, in the copolymer, as a result of the stretching vibration of C=N bonds in diiminoquinoid ring and skeletal vibration of the benzenoid aromatic ring, respectively.<sup>[15]</sup> It is found that the absorption due to quinoid ring results in higher wavenumbers and its intensity declines as EA feed content decreases; this suggests that this absorption results mainly from the EA unit. Therefore the diiminoquinoid structure in the AQ/EA copolymer is mainly from the EA units. The peak at 1500  $\text{cm}^{-1}$  shifts to higher wavenumbers with an increase in AQ content, but its intensity almost remains constant. When AQ feed content is more

than 20 mol%, a new absorption peak appears at 1559  $\text{cm}^{-1}$  that should correspond to in-plane bending vibration of N–H in secondary amine group in AQ units.<sup>[14]</sup> This peak might overlap by the stretching vibration peak of C=N bonds in diiminoquinoid ring when AQ content is low.<sup>[15]</sup> The medium absorption peak centered at 1314–1308  $\text{cm}^{-1}$  gets weaker with reducing EA content and therefore is ascribed to the C–N stretching vibration in the EA quinoid–imine units.<sup>[15]</sup> It also proves that the EA units in the copolymer exist as more quinoid structure. The peak at 1145  $\text{cm}^{-1}$  from C–H in-plane bending vibration of the 1,2,4-trisubstituted benzene ring gets stronger with increasing EA unit content; this indicates that the peak is attributed to EA units. The existence of the trisubstituted EA units and secondary amino groups verifies the formation of polymers.

The IR spectra of AQ/EA (10:90) copolymers formed in a polymerization temperature range of 5–35°C or in the three above-mentioned media seem similar to each other, implying similar copolymer structure. Therefore, the polymerization temperature and medium have a weak influence on the molecular structure of the AQ/EA copolymer.

**UV/Vis spectra of the AQ/EA copolymers:** UV/Vis spectra of the AQ/EA copolymer bases with seven AQ/EA ratios are

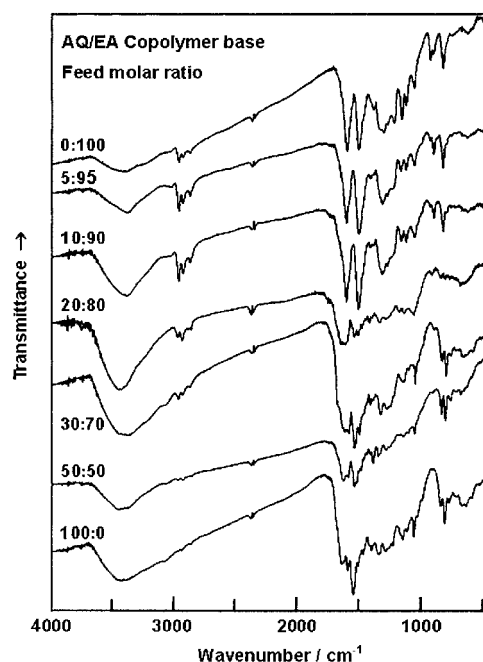


Figure 4. IR spectra of 8-aminoquinoline (AQ)/2-ethylaniline (EA) copolymer bases prepared in 1 M HCl at 5°C with AQ/EA feed molar ratios of 0:100, 5:95, 10:90, 20:80, 30:70, 50:50 and 100:0.

systematically shown in Figure 5. A strong band and a broad but relatively weak band can be observed in the UV/Vis spectra. When AQ feed content is less than 10 mol%, the strong absorption band around 306 nm (band I) is assigned to  $\pi-\pi^*$  transition of benzenoid ring, and the weak band around 613 nm (band II) is attributed to excitation transition from benzenoid ring to quinoid ring.<sup>[16]</sup> Both transitions are related to the extension of the conjugation along the molecular chain. The red shift of absorption band indicates a more extended conjugating system, which is assigned to longer polymer chain, suggesting higher molecular weight of the polymer and more quinoid structure. Both bands I and II show hypsochromic shifts to 263–290 and 478–481 nm when AQ feed content is more than 20 mol%; this indicates a diminution in the extension of the conjugation system along the molecular chain, maybe due to the lowering of the molecular weight. As seen in Table 3, excitation transition of AQ/EA copolymer shifts to shorter wavelength with increasing AQ content, implying shorter extension of quinoid structure, that is, less quinoid content in the more AQ unit-containing copolymer. This behavior is in accord with the IR spectral results. It can also be seen from Table 3 that both of the absorption bands of AQ/EA (10:90) copolymers obtained at a higher temperature or in a higher pH medium show a shift to short wavelength, implying shorter conjugating length, that is, lower molecular weight. Note that at a fixed polymerization temperature of 5 °C the AQ/EA (10:90) copolymer exhibits a maximal intensity ratio of band II over I. This is also an indication of the strong interaction between AQ and EA monomers. The AQ/EA (10:90) copolymer formed at 15 °C exhibits the highest intensity ratio of band II over I, probably owing to the optimal copolymerizability, implying that 15 °C is the optimal polymerization temperature for the synthesis of the AQ/EA (10:90) copolymer with the longest conjugation length. This result is coincident with the maximal polymerization yield in Figure 2.

#### <sup>1</sup>H NMR spectra and gel permeation chromatograph (GPC) of the AQ/EA copolymers: 500 MHz <sup>1</sup>H NMR spectra of

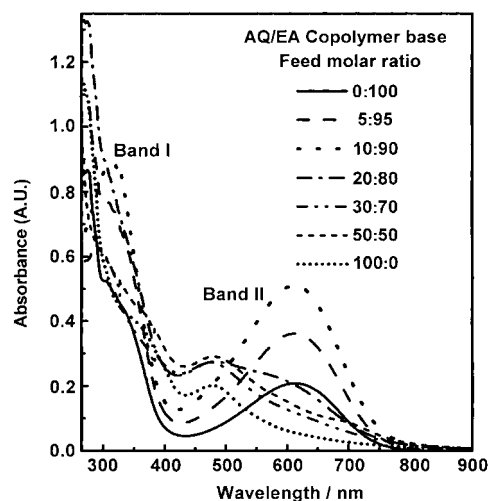


Figure 5. UV/Vis spectra of the solution AQ/EA copolymer bases prepared at 5 °C in 1 M HCl with AQ/EA feed molar ratios of 0:100, 5:95, 10:90, 20:80, 30:70, 50:50 and 100:0 at a concentration of 12.5 mg L<sup>-1</sup> in NMP.

seven AQ/EA copolymer bases in the complete composition range are characterized by five main signals, corresponding to five types of protons, respectively. There is a strong distinct peak centered at 1.1 ppm and a relatively weaker peak at 2.6 ppm. Both of the peaks become stably weaker as the EA unit content declines, indicating that they exactly correspond to  $-\text{CH}_3$  and  $-\text{CH}_2-$  protons on the EA units, respectively. The weak peaks from 5.1 to 6.0 ppm might correspond to the protons of primary amino groups at the  $-\text{NH}_2$  end group of polymer chain. The weak and broad peaks in a wide range from 6.2 to 9.7 ppm are assigned to the aromatic protons on AQ and EA units. On the basis of an area comparison of the aromatic proton peak (6.2–9.7 ppm) on AQ and EA units with  $-\text{CH}_3$  proton peak (1.1 ppm) on EA unit, it is possible to calculate the actual AQ/EA molar ratio of the copolymers. The number of aromatic protons on AQ units might be calculated through the following equation:

Table 3. UV/Vis spectra (in NMP), solubility, and solvatochromism of 8-aminoquinoline (AQ)/2-ethylaniline (EA) copolymer bases prepared at different polymerization conditions.

AQ/EA molar ratio	Polymerization <i>T</i> / °C	Polymerization medium	Band I/II wavelength / nm	Intensity ratio of band II over I	Solubility <sup>[a]</sup> and solution color <sup>[b]</sup>			
					DMSO (7.2) <sup>[c]</sup>	NMP (6.7) <sup>[c]</sup>	CHCl <sub>3</sub> (4.1) <sup>[c]</sup>	THF (4.0) <sup>[c]</sup>
0:100	5	1 M HCl	306/614	0.40	S, B	PS, BB	MS, BP	PS, P
5:95	5	1 M HCl	306/612	0.47	S, B	S, B	S, BP	PS, BP
10:90	5	1 M HCl	312/612	0.57	S, B	S, BB	S, BP	PS, BP
20:80	5	1 M HCl	274/481	0.21	S, PB	S, PB	S, P	S, PB
30:70	5	1 M HCl	290/474	0.42	MS, Br	S, RB	SS	SS
50:50	5	1 M HCl	263/480	0.27	PS, Br	S, RB	SS	SS
100:0	5	1 M HCl	267/478	0.18	PS, RB	PS, RB	IS	IS
10:90	15	1 M HCl	310/611	0.60	S, B	S, B	S, BP	S, B
10:90	25	1 M HCl	308/608	0.52	S, B	S, B	S, BP	S, B
10:90	35	1 M HCl	308/608	0.49	S, B	S, B	S, GB	S, B
10:90	25	0.5 M H <sub>2</sub> SO <sub>4</sub>	315/594	0.53	S, B	S, B	S, PB	S, BP
10:90	25	MeCN + H <sub>2</sub> O <sup>[d]</sup>	288/550	0.39	S, P	S, P	S, P	S, P

[a] IS: insoluble; MS: mainly soluble; PS: partially soluble; S: soluble; SS: slightly soluble. [b] B: blue; BB: bluish black; BP: bluish purple; Br: brown; GB: greenish blue; P: purple; PB: purplish brown; RB: reddish brown. [c] Polarity index of the solvents. [d] Volume ratio of MeCN/H<sub>2</sub>O 2:1.

$$\begin{aligned} \text{AQ proton area} &= \\ \text{total aromatic proton area} - \text{methyl proton area} & \quad (2) \end{aligned}$$

Therefore,

$$\begin{aligned} \text{molar ratio of AQ to EA} &= \\ (\text{AQ proton area}/5)/(\text{methyl proton area}/3) & \quad (3) \end{aligned}$$

The number-average degree of polymerization of AQ/EA copolymer would be roughly calculated according to the area comparison of the resonance peaks of -NH- over -NH<sub>2</sub> groups by the following equation:

$$\begin{aligned} (\text{DP})_n &= [2 \times (-\text{NH}- \text{ proton area}) \\ + (-\text{NH}_2 \text{ proton area})/2]/[(-\text{NH}_2 \text{ proton area})/2] & \quad (4) \end{aligned}$$

The results calculated in this way are listed in Table 1. The genuine AQ content of the copolymer seems higher than feed AQ content, implying that AQ monomer inclines to homopolymerize rather than copolymerize with EA monomer. On the contrary, EA monomer inclines to copolymerize with AQ monomer rather than homopolymerize. It is observed that the AQ monomer is relatively advantageous for the formation of the radical cation at the growing chain end to maintain active in comparison with EA monomer. The higher electron density on the AQ quinoline ring induces the AQ radical cation more stable than EA radical cation and accordingly provides it longer lifetimes for the chain propagation. Furthermore, the quinoline ring with higher electron density than EA benzene ring is more easily attacked by the radical cation, resulting in an easier electrophilic aromatic substitution. Both of the factors induce a largely increased AQ content in the copolymer compared to AQ feed content<sup>[17]</sup> and an enlarged degree of polymerization. The degree of polymerization rises first and then reduces with an increase in AQ content. AQ/EA (10:90) copolymer possesses the maximal degree of polymerization because of the above-mentioned two factors. Again, the larger steric hindrance of AQ ring leads to decreased formation of the longer polymer chain in the case of higher AQ content.

The results from the GPC analysis suggest that the THF soluble part of AQ/EA (10:90) copolymer base also exhibits the highest molecular weight. The number-average molecular weight rises slightly from 2923, 3202 to 3211 as AQ feed content increases from 0, 5 to 10 mol%. In addition, the AQ/EA copolymers exhibit a single peak of molecular-weight distribution with the polydispersity index from 2.04 to 3.14. Notably the molecular weight of the polymers obtained by GPC is lower than that determined by NMR spectroscopy because different solvents were used for the measurements. Therefore, the THF soluble part of the polymer base should exhibit lower molecular weight than the completely soluble polymer in DMSO.

**Size of fine particles of the AQ/EA copolymers:** Generally, an external stabilizer is essential for the formation of nano-

particles through polymerization. It has been reported that the PAN particles with an average diameter of around 15 μm were formed in situ by the oxidative polymerization without the external stabilizer.<sup>[18]</sup> By incorporating sulfonic and methoxy groups at the PAN chain as internal stabilizer, sub-micrometer particles of sulfonic alkoxy aniline polymer with a mean diameter around 218 nm have been fabricated in situ by the oxidative polymerization.<sup>[18]</sup> Herein, we suggest that both the particle size and its distribution of AQ/EA copolymers analyzed by Laser Particle Size Analyzer (LPSA) exhibit a significant dependency on the AQ/EA ratio, as shown in Figure 6. The number-average diameter

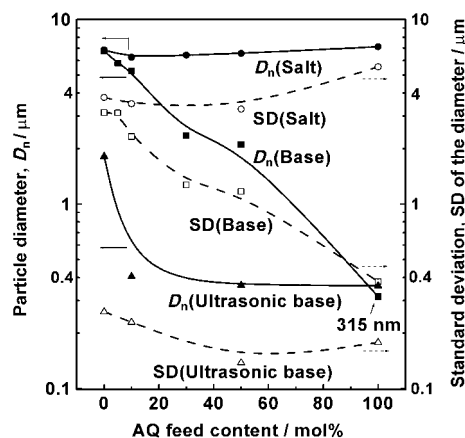
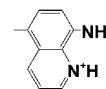


Figure 6. Particle size and its distribution of 8-aminoquinoline (AQ)/2-ethylaniline (EA) copolymer particles in water with different AQ feed contents obtained in HCl (1 M) at 5 °C.

(*D<sub>n</sub>*) of the virgin copolymer salts ranges from 6.243 to 7.121 μm. Both the *D<sub>n</sub>* and its standard deviation of the base particles dramatically decrease from 6.761 μm to 315 nm and from 3.131 μm to 380 nm, respectively, after a dedoping treatment in NH<sub>4</sub>OH. Therefore, a transformation of the copolymer state from virgin salt to emeraldine base leads to much smaller particle size, particularly at a higher AQ content. This decrease in particle size would be attributed to the removal of external dopants (i.e., HCl) of the copolymer chains; this induces a tight arrangement of copolymer chains and further decreased size of the copolymer base particles. In addition, the lone electron pair on the AQ ring-nitrogen can combine with -N<sup>+</sup>H= in the Scheme 1 to enable the for-



Scheme 1. Positively charged quaternary ammonium structure on the AQ unit.

mation of the copolymer chains with positive charge. An electrostatic repulsion between the positive charges makes the chains less likely close and therefore retains the low accumulation of the copolymer particles. The higher the AQ

content, the greater the static rejection between copolymer chains, which results in a much smaller particle size. Noteworthy, the  $D_n$  of fine particles of AQ homopolymer base is only 315 nm that drops into a sub-micrometer order of magnitude.

Figure 7 illustrates a remarkable influence of AQ/EA polymerization temperature on the particle size of the copolymer. The  $D_n$  of the AQ/EA (10:90) copolymer particles decreases from 6.243  $\mu\text{m}$  to 3.287  $\mu\text{m}$  for virgin salt and from 5.252  $\mu\text{m}$  to 348 nm for emeraldine base when increasing the polymerization temperature from 5 to 35  $^{\circ}\text{C}$ . The decrease of the  $D_n$  of the particles at increasing polymerization temperatures may be primarily assigned to an increase in AQ unit content in the copolymer because the polymerizability of AQ monomer might be enhanced at an elevated temperature as compared with the EA monomer. The decreased electroconductivity of the copolymer as discussed in Figure 2 could be another evidence of an increased AQ content. Similarly, dedoping process can also decrease the  $D_n$  of the AQ/EA copolymer particles obtained in different reaction media, as listed in Table 2. However, the three media used in the copolymerization have a minor influence on the  $D_n$ . Possibly, the particle size does not seem to depend greatly on the surrounding anions.

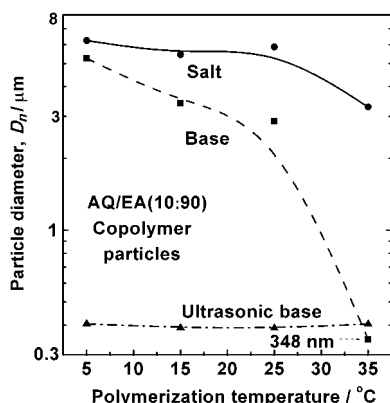


Figure 7. The effect of polymerization temperature on the particle size of 8-aminoquinoline (AQ)/2-ethylaniline (EA) (10:90) copolymer particles in water obtained in HCl (1M).

Interestingly after an ultrasonic dispersion the copolymer base particles prepared with various comonomer ratios and at different polymerization temperatures exhibit almost uniform  $D_n$  in a narrow scale from 361 to 405 nm, as shown in Figures 6 and 7, except for the particles of EA homopolymer. This novel behavior may be ascribed to the stabilizing function of the static repulsion between the AQ/EA copolymer chains because of the presence of positively charged quaternary ammonium structures on the AQ units. That is to say, fine AQ/EA copolymer particles with similar  $D_n$  but different structure and properties can be prepared under various polymerization conditions. Before the ultrasonic dispersion, the copolymer particles coalesce with each other in order to reduce their surface area and then surface

energy, resulting in agglomerates of the copolymer particles. When these agglomerates were scattered by ultrasonic treatment, the positive quaternary ammonium structures on the surface of copolymer chain coils can act as internal stabilizers due to their interchain electrostatic repulsion, thus leading to fine particles with a uniformly sub-micrometer dimension between 361 and 405 nm. Because there is no quaternary ammonium structure in the EA homopolymer chains as internal stabilizer, the EA homopolymer particles easily coalesce together again after an ultrasonic scattering and the sub-micrometer particles are unable to exist stably.

A detailed atomic force microscopy (AFM) observation further reveals the size and shape of the AQ/EA copolymer base particles. The particles of copolymer bases appear to be of an ellipsoid shape rather than a sphere, as shown in Figure 8a–c. The ultrasonic ellipsoidal particles of AQ/EA (10:90), (50:50), and (100:0) copolymers have major/minor axis diameter of 87/72, 80/67, and 24/14 nm, respectively. The variation of the particle size with AQ/EA ratio revealed by AFM is similar to that by LPSA in Figure 6. Traditionally, nanoparticles are prepared through an emulsion polymerization in which stabilizer, emulsifier or dispersant are indispensable, which complicates the predictability of nanoparticles. In this study, the AQ/EA copolymer nanoparticles are simply prepared by chemical oxidative polymerization without additives. Furthermore, the nanoparticles formed by the emulsion polymerization are usually spherical, whereas herein we synthesized ellipsoidal and pure nanoparticles by the chemical oxidation precipitation polymerization. It can also be seen from the AFM and transmission electron microscopy (TEM) images, Figures 8d, e and 9, of the ultrasonic particles of AQ/EA (10:90) copolymer formed at three polymerization temperatures, that the particle size also depends on the polymerization temperature, different from Figure 7.

It should be evidently noted that the particle size of the three polymers revealed by AFM and TEM is much smaller than that determined by LPSA. The smaller particle size observed by AFM and TEM must be attributed to contraction and compaction of the particles because of the elimination of water inside the particles during the drying process.<sup>[18]</sup> In other words, microscopic samples are equilibrium dry state in ambient air for AFM observation and very dry state in high vacuum for TEM observation while LPSA samples are swollen in water.

**Bulk electrical conductivity of the AQ/EA copolymers:** The AQ/EA copolymers exhibit an electrical semi-conductivity like other nitrogen heterocyclic aromatic amine polymers. The electrical conductivity of the copolymers obtained is shown in Figures 1, 2 and Table 2. It seems that the copolymer base particles in the whole composition range have a conductivity of the magnitude from  $10^{-11}$  to  $10^{-8} \text{ Scm}^{-1}$ .<sup>[19]</sup> After doped by 1 M HCl aqueous solution for 48 h, the conductivity of the redoped salts of the copolymer particles remarkably increases up to between  $10^{-7}$  and  $10^{-5} \text{ Scm}^{-1}$ .<sup>[20]</sup> In particular, the AQ/EA (10:90) copolymer exhibits the sharp-

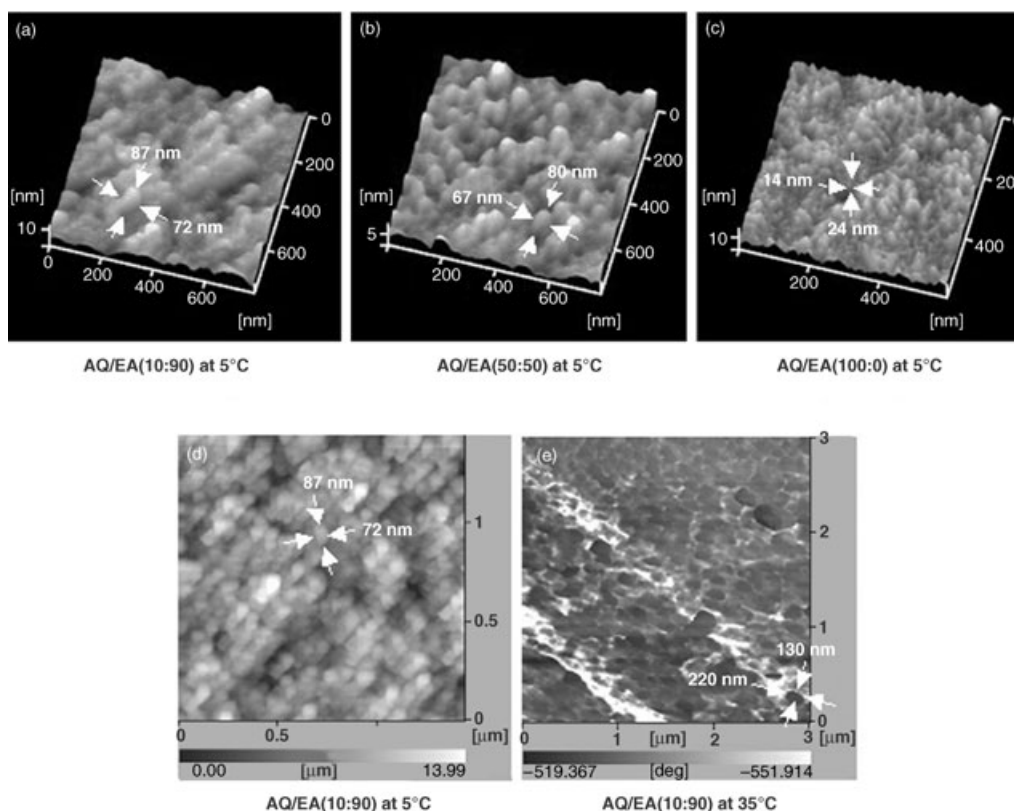


Figure 8. AFM 3D images of a) AQ/EA (10:90), b) (50:50) and c) (100:0) copolymer base particles at the polymerization temperature of 5°C as well as topographic image of AQ/EA (10:90) copolymer base particles at the polymerization temperature of d) 5°C, e) 35°C obtained in the polymerization medium of HCl (1 M) and then treated ultrasonically.

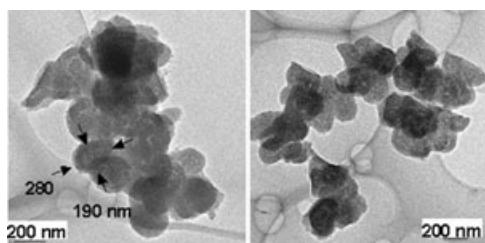


Figure 9. TEM images of 8-aminoquinoline/2-ethylaniline (10:90) copolymer base particles obtained in HCl (1 M) at 25°C and then treated ultrasonically.

est conductivity rise and also the maximal conductivity in the six AQ/EA polymers upon redoping,<sup>[17]</sup> because of its highest molecular weight (see also Table 1). This phenomenon indicates that the conductivity of redoped copolymers is mainly determined by the doping state and molecular weight. Notably the AQ/EA (50:50) copolymer salt exhibits the lowest conductivity owing to a combination of higher AQ unit content and more irregular copolymer backbone structure<sup>[13]</sup> which results in the most disorder packing of the copolymer chains.

It can be concluded from Figure 2 that the electrical conductivity of HCl doped AQ/EA (10:90) copolymer increases with lowering polymerization temperature, possibly due to

an increased molecular weight of copolymer at lower temperature. The HCl redoped AQ/EA copolymer prepared in HCl medium exhibits the highest conductivity, while the HCl redoped copolymer prepared in the mixture of MeCN and water is an insulator, as listed in Table 2. In summary, the comonomer ratio, polymerization condition and doping degree could be all utilized to efficiently control and regulate the conductivity of the copolymers to some extent.

#### Solubility and solvatochromism of the AQ/EA copolymers:

On the basis of a careful comparison of the solubility of the copolymer base particles in four typical solvents with different polarity indexes in Table 3, it can be seen that the solubility is greatly influenced by AQ/EA molar ratio but almost not polymerization temperature and medium. The copolymer exhibits a reduced solubility in all the four solvents as the AQ content increases. When AQ feed content is not lower than 30 mol %, the copolymers are slightly soluble or insoluble in THF and CHCl<sub>3</sub>, regardless of their relatively low molecular weight. This implies that the poor solubility of the copolymer bases with high AQ content may be primarily attributed to a high chain rigidity of the polymers caused by many AQ units. Other nitrogen heterocyclic aromatic amine polymers also demonstrate a similar phenomenon.<sup>[1,3]</sup> The copolymer bases containing AQ feed content of 5–50 mol % are totally soluble in NMP but both EA and



AQ homopolymers are only partially soluble in NMP, as well as the copolymer bases containing AQ feed content of 5–20 mol% are totally soluble in  $\text{CHCl}_3$  but other AQ/EA polymers are mainly soluble or even insoluble in  $\text{CHCl}_3$ . This means that the copolymers formed by the oxidative copolymerization are genuine copolymers containing both AQ and EA units rather than a mixture of two respective homopolymers.<sup>[17]</sup>

A significant variation of the AQ/EA copolymer solution color with the solvents is testified, that is, a unique solvatochromic behavior. It is seen from Table 3 that the copolymer solution displays different colors in various solvents. The AQ/EA copolymer with AQ feed content of less than 20 mol% is blue in NMP and DMSO and displays a tendency to violet in THF and  $\text{CHCl}_3$ . At an AQ feed content of more than 20 mol%, the corresponding copolymer solution looks like a brownish color. It indicates that the AQ/EA copolymer solution reflects homochromous light of longer wavelength in NMP and DMSO than in THF and  $\text{CHCl}_3$ . That is, the copolymer solution returns back homochromous light of longer wavelength in solvents with strong polarity, whereas reverberates that of shorter wavelength in solvents with weak polarity. The AQ/EA copolymer solution prepared at different polymerization temperatures or media confirms the phenomenon that the copolymer solution color is dependent on the solvent polarity, as indicated in Table 3. This appears to reveal the fact that the copolymer chains are relatively extended in highly polar DMSO and NMP.

**Film formability of the AQ/EA copolymers:** Although the film formability is one of the most important processing abilities for the new practical polymers, it seems that few reports on the solution-casting film formability of AQ polymers are found till now. Here we report a film-forming ability of AQ/EA copolymer bases prepared by chemical oxidative polymerization with NMP as a solvent. It is discovered that AQ/EA (5:95 and 10:90) copolymer bases obtained at polymerization temperature of 5 °C exhibit excellent film formability.<sup>[16]</sup> The resulting films adhesive strongly to glass and display shining bright color caused by a very smooth surface without defects.<sup>[18,21]</sup> The AQ/EA (10:90) copolymer bases synthesized at 15–35 °C or in 0.5 M  $\text{H}_2\text{SO}_4$ , or in a MeCN/ $\text{H}_2\text{O}$  mixture also display good film formability, the films of which are smooth and flat but have relatively pale gloss. However, the film formability of the copolymer bases with the AQ feed content of higher than 10 mol% is not satisfied. It appears that a good solubility does not always mean good film formability. The good film formability of AQ/EA (10:90) copolymer bases could be assigned to higher molecular weight.<sup>[21]</sup> Another possible reason should be due to the formation of a real solution, where the copolymer chains could dissolve uniformly in the solvent rather than a system with solid or swollen polymer fine particles scattered in the solvent appearing as a solution to naked eyes.

## Conclusion

A simple chemical oxidative copolymerization of AQ and EA monomers was successfully carried out. The copolymerization yield, macromolecular and morphological structures, electrical conductivity, solubility, solvatochromism, and film formability of the AQ/EA copolymer particles vary largely with the AQ/EA ratio, polymerization temperature and medium. This indicates that the copolymerization characteristics, structure and properties of the copolymers could be controlled or even optimized by choosing AQ/EA ratio and polymerization conditions. EA monomer is readily oxidized to initiate the polymerization in comparison with AQ monomer, while AQ monomer with high electron density on the quinoline ring would stabilize the activated end group and easily enable electrophilic aromatic substitution, leading to high AQ content in the resulting copolymer chain as compared with correspondent feed content. The AQ/EA copolymer exhibits the upmost molecular weight, electrical conductivity, and film formability at the AQ feed content of 10 mol%, yet the copolymer exhibits the undermost polymerization yield and conductivity at the AQ feed content of 50 mol%. A non-monotonic variation of the oxidation potential, OCP, and polymerization yield of the monomers as well as UV/Vis spectrum and electroconductivity of the copolymers with AQ/EA ratio indicates a strong interaction between AQ and EA monomers. Specifically, a genuine copolymerization between both monomers has occurred. Both low temperature and low pH medium are favorable for the formation of the AQ/EA copolymers with high molecular weight. The particle size of AQ/EA copolymers could be considerably controlled by optimizing the monomer ratio, alkaline treatment, and polymerization temperature. The mean diameter of the AQ/EA copolymer base particles decreases steadily with enhancing AQ content or polymerization temperature. AFM observation reveals the formation of nano-ellipsoids with the major/minor axis diameter of respective 24/14 nm and 80/67 nm of the particles of AQ homopolymer and AQ/EA (50:50) copolymer prepared at 5 °C in 1 M HCl as polymerization medium for the first time. The copolymer nanoparticles with the diameter of smaller than 90 nm can be simply obtained by an ultrasonic dispersion. A simple method of in situ polymerization to prepare pure nanoparticles of the AQ/EA polymers without adsorptive stabilizer or interior sulfonic group is demonstrated. The AQ units with positively charged quaternary ammonium groups are vital for the formation and stable existence of the nanoparticles.

## Experimental Section

8-Aminoquinoline (AQ), 2-ethylaniline (EA), ammonium persulfate  $[(\text{NH}_4)_2\text{S}_2\text{O}_8]$ , HCl,  $\text{H}_2\text{SO}_4$ , acetonitrile (MeCN), dimethylsulfoxide (DMSO), *N*-methylpyrrolidone (NMP), chloroform ( $\text{CHCl}_3$ ), and tetrahydrofuran (THF) were commercially obtained as chemical pure reagents and used without further purification.

**Preparation of the fine particles of the copolymers:** A representative process for the synthesis of the AQ/EA (10:90) copolymer particles is: to HCl aqueous solution (1 M, 10 mL) in a glass flask in water-bath at 5°C was added AQ (0.147 g, 1 mmol) and EA (1.14 mL, 9 mmol) and then stirred vigorously for half an hour. An oxidant solution was prepared separately by dissolving ammonium persulfate (2.327 g, 10 mmol) in HCl aqueous solution (1 M, 5 mL). The monomer solution was then treated with the oxidant solution by dropwise adding the oxidant solution at a rate of one drop per three seconds. The reaction mixture was stirred continuously for 10 h at 5°C together with the measurement of the OCP and temperature of the polymerization solution. After that, the copolymer HCl salt particles as precipitates were isolated from the reaction mixture by filtration and washed with an excess of distilled water in order to remove the remaining oxidant and water-soluble oligomer. The HCl salt was subsequently neutralized in ammonium hydroxide (0.2 M, 100 mL), stirring overnight. The final fine polymer particles were left to dry in ambient air for one week, obtaining the emeraldine base of AQ/EA (10:90) copolymer as black solid powders.

When using MeCN/water as polymerization medium, AQ/EA monomers were added to MeCN (10 mL). An oxidant solution was prepared separately by dissolving ammonium persulfate in distilled water (5 mL). Other process is exactly the same as above.

**Measurements:** Cyclic voltammetric measurements were performed by using Model 660a Electrochemical Workstation (CH Instruments) with correspondent electrochemical system software. Two platinum (Pt) foils with the area of 1 cm<sup>2</sup> were used as working electrode and counter electrode. SCE was used as reference electrode. Oxidation potential of AQ, EA and AQ/EA (50:50) mixture was examined by cyclic voltammetry at a sweep rate of 50 mV s<sup>-1</sup> on Pt electrode in 0.5 M H<sub>2</sub>SO<sub>4</sub> aqueous solution and 0.1 M NaClO<sub>4</sub>/MeCN solution containing 10 mM AQ, 10 mM EA and 5 mM AQ/5 mM EA, respectively. The AQ/EA copolymerization was followed by the OCP profile technique, using a potentiometer equipped with an SCE as reference electrode and a Pt electrode as a working electrode. The measurement set-up of the OCP is designed to attain an equilibrium situation, where both anodic and cathodic reactions proceed at an equal finite rate.<sup>[10]</sup> The net current between both electrodes is zero and the voltage corresponding to this zero current is defined as the OCP. The bulk electrical conductivity of the salt and base of the copolymer particles was measured by the following plan: put copolymer powders (10 mg) between two round-disk stainless iron electrodes with a diameter of 1 cm and press the powder tight to a pellet, and then measure the resistance and thickness of the copolymer pellet with a multimeter and a thickness gauge, respectively. The redoped salt samples were prepared by doping the copolymers with 1 M HCl aqueous solution for 48 h. The copolymer solubility was evaluated as follows: polymer powder (2 mg) was added to 1 mL solvent and dispersed drastically after shaking intermittently for 2 h at ambient temperature. The film formability was evaluated with NMP as solvent at a fixed copolymer concentration (10 g L<sup>-1</sup>) by a solution casting method. The NMP in copolymer solution on glass with the area of 3 × 3 cm<sup>2</sup> was evaporated at around 70°C.

IR spectra were recorded on a Nicolet Magna-IR 550 spectrometer at 2 cm<sup>-1</sup> resolution on KBr pellets. High resolution <sup>1</sup>H NMR spectra were obtained in deuterated [D<sub>6</sub>]DMSO by using Bruker DMX 500 spectrometer operating at 500.13 MHz. UV/Vis spectra of a homogeneous solution of AQ/EA copolymer bases at a certain concentration (12.5 mg L<sup>-1</sup>) in NMP were recorded on Perkin-Elmer Instruments Lambda 35 in a range of 1100–190 nm at a scanning rate of 480 nm min<sup>-1</sup>. Molecular weight of the AQ/EA copolymers was measured using HP1100 GPC column (PL-

gel mixed C × 2, PL gel 50 nm) and THF as solvent and mobile phase as well as monodisperse polystyrene (*M*<sub>w</sub> 500–10<sup>6</sup> g mol<sup>-1</sup>) as standard. The size and its distribution of the copolymer particles formed just after polymerization or dedoping treatment were analyzed with water as mobile phase on Beckman Coulter LS230 LPSA. The dry copolymer particles were observed by an SPA-300HV AFM system, Seiko SII Instruments, Japan and Jeol JEM-2010 high resolution TEM.

## Acknowledgements

The authors would like to thank Prof. Dr. Roy G. Gordon in Department of Chemistry and Chemical Biology of Harvard University for his valuable help. The project is supported by the National Natural Science Foundation of China (20174028).

- [1] X. G. Li, M. R. Huang, Y. Jin, Y. L. Yang, *Polymer* **2001**, *42*, 3427.
- [2] a) L. I. Belousova, N. N. Vlasova, Y. N. Pozhidaev, M. G. Voronkov, *Russ. J. Gen. Chem.* **2001**, *71*, 1879; b) S. Majid, M. E. Rhazi, A. Amine, A. Curulli, G. Palleschi, *Microsc. Acta* **2003**, *143*, 195.
- [3] X. G. Li, M. R. Huang, F. Li, W. J. Cai, Z. Jin, Y. L. Yang, *J. Polym. Sci. Part A Polym. Chem.* **2000**, *38*, 4407.
- [4] H. A. A. El-Rahman, J. W. Schultze, *J. Electroanal. Chem.* **1996**, *416*, 67.
- [5] T. C. Wen, Y. H. Chen, A. Gopalan, *Mater. Chem. Phys.* **2002**, *77*, 559.
- [6] H. An, M. Seki, K. Sato, K. Kadoi, R. Yosomiya, *Polymer* **1989**, *30*, 1076.
- [7] F. R. Diaz, C. O. Sanchez, M. A. D. Valle, J. L. Torres, L. H. Tagle, *Synth. Met.* **2001**, *118*, 25.
- [8] X. G. Li, L. X. Wang, M. R. Huang, Y. Q. Lu, M. F. Zhu, A. Mener, J. Springer, *Polymer* **2001**, *42*, 6095.
- [9] A. L. Schemid, L. M. Lira, S. I. Cordoba de Torresi, *Electrochim. Acta* **2002**, *47*, 2005.
- [10] Y. Wei, K. F. Hsueh, G. W. Jiang, *Polymer* **1994**, *35*, 3572.
- [11] X. G. Li, W. Duan, M. R. Huang, Y. L. Yang, D. Y. Zhao, *Polymer* **2003**, *44*, 6273.
- [12] N. Gospodinova, L. Terlemezyan, *Prog. Polym. Sci.* **1998**, *23*, 1443.
- [13] K. Naoi, S. Suematsu, A. Manago, *Electrochim. Acta* **2002**, *47*, 1091.
- [14] K. A. Shaffie, *J. Appl. Polym. Sci.* **2000**, *77*, 988.
- [15] A. Abdel-Azzem, U. S. Yousef, G. Pierre, *Eur. Polym. J.* **1998**, *34*, 819.
- [16] W. Wei, W. W. Focke, G. E. Wnek, A. Ray, A. G. MacDiarmid, *J. Phys. Chem.* **1989**, *93*, 495.
- [17] X. G. Li, M. R. Huang, Y. M. Hua, M. F. Zhu, Q. Chen, *Polymer* **2004**, *45*, 4693.
- [18] X. G. Li, M. R. Huang, W. Feng, M. F. Zhu, Y. M. Chen, *Polymer* **2004**, *45*, 101.
- [19] A. G. MacDiarmid, *Angew. Chem.* **2001**, *113*, 2649; *Angew. Chem. Int. Ed.* **2001**, *40*, 2581.
- [20] Z. X. Bao, C. X. Liu, P. K. Kahol, N. J. Pinto, *Synth. Met.* **1999**, *106*, 107.
- [21] X. G. Li, M. R. Huang, Y. Q. Lu, M. F. Zhu, *J. Mater. Chem.* **2005**, *15*, 1343.

Received: November 11, 2004

Published online: May 4, 2005